J Fluoresc (2008) 18:1199–1205
DOI 10.1007/s10895-008-0378-2

SHORT COMMUNICATION

Thioflavin T Displays Enhanced Fluorescence Selectively Inside Anionic Micelles and Mammalian Cells

Satish Kumar · Atul K. Singh · G. Krishnamoorthy · Rajaram Swaminathan

Received: 27 January 2008 / Accepted: 21 April 2008 / Published online: 28 May 2008

Abstract Thioflavin T (ThT) has been widely employed to detect amyloid fibrils in tissues and recently in presence of SDS micelles. However, the contribution of membranes or micelles to ThT fluorescence has never been investigated. In this paper, we show for the first time that the anionic micellar microenvironment of SDS has a profound impact on the absorption and fluorescence spectra of ThT in sharp contrast to cationic (CTAB) and neutral micelles (Triton X-100 & Tween 20). Unlike CTAB or Triton X-100 or Tween 20 micelles, formation of SDS micelles shifts the λ_{max} for ThT absorption from 412 nm in buffer to 428 nm inside the micelle, with a 28% increase in the peak molar absorptivity and a ~13 fold increase in ThT fluorescence (λ_{max}= 489 nm). Extending these observations to cell plasma membranes, we show that ThT can quickly enter and appear selectively fluorescent inside mammalian cells like *BHK21* and *HT29*, against a dark background owing to negligible fluorescence from free ThT in aqueous medium. The above results suggest that ThT can be a useful probe for live cell imaging and for selectively labeling micelles on the basis of the charge in the polar headgroup.

Keywords Surfactants · Spectroscopy · Pyrene · Amyloid fibrils · Mammalian cells · SDS

Abbreviations

ThT	thioflavin T
HEWL	hen eggwhite lysozyme
PBS	phosphate buffered saline

Introduction

Thioflavin T (ThT), a positively charged benzothiazole dye (Fig. 1), has been extensively employed to detect the presence of amyloid fibrils in aggregated proteins [1–4]. Apart from proteins, ThT has been shown to be fluorescent when bound to DNA [5, 6] and cyclodextrins [7] also.

ThT displays a large increase in fluorescence when bound to amyloid fibrils in comparison to free ThT under identical conditions [4]. The mechanism behind this increase in fluorescence is not fully understood. It has been hypothesized to arise from the restricted torsional relaxation between benzthiazole ring and benzene ring when ThT is bound to amyloid fibrils, which would otherwise favor the non-radiative pathway when rotation is freely possible [8, 9]. The quantum yield of ThT has been shown to increase dramatically when the dye is located in a viscous environment [10]. Thus a viscous or a rigid microenvironment is likely to enhance the fluorescence of ThT. Recently it was shown that absorption spectrum of ThT is sensitive to the surrounding solvent polarity, where the peak in long

Electronic supplementary material The online version of this article (doi:10.1007/s10895-008-0378-2) contains supplementary material, which is available to authorized users.

S. Kumar · R. Swaminathan (✉)
Department of Biotechnology,
Indian Institute of Technology Guwahati,
Guwahati 781039 Assam, India
e-mail: rsw@iitg.ernet.in

G. Krishnamoorthy
Department of Chemistry,
Indian Institute of Technology Guwahati,
Guwahati 781039 Assam, India

A. K. Singh
Department of Biotechnology,
Indian Institute of Technology Kharagpur,
Kharagpur 721302, India

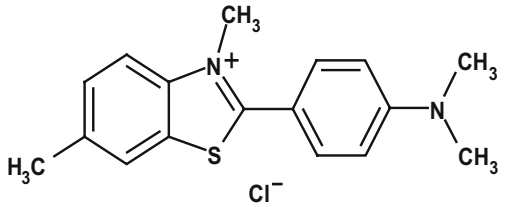

Fig. 1 The structure of thioflavin T

wavelength absorption band shifts from 412 nm in water to 424 nm in chloroform [11].

We reasoned that a rigid microenvironment can be provided in the interior of a cell membrane too. Incidentally, ThT has been employed to detect amyloid in tissue sections, where it also binds to other tissues like cartilage matrix, elastic fibers and mucopolysaccharides [1, 12]. Moreover, several reports suggesting amyloid formation in the presence of SDS (near cmc) have appeared [13, 14], making it imperative to investigate the influence of SDS micelles alone on ThT. To the best of our knowledge, the interaction of ThT with membranes or micelles has NEVER been studied. In this work we initially investigated the influence of different surfactant micelles on the absorption and fluorescence spectra of ThT. Later to study the influence of biomembranes, we added ThT to cultures of live eukaryotic cells also. Our results show that in contrast to cationic and neutral micelles, the anionic micellar microenvironment of SDS has a dramatic influence on Thioflavin T absorption and fluorescence spectra. In addition the facile entry and subsequent fluorescence of thioflavin T inside mammalian cells has potential applications for this molecule as a membrane-permeant probe for cell labeling.

Experimental

Materials

Hen egg white lysozyme (HEWL), Thioflavin T, Gly-Gly. HCl, Tween 20 and pyrene were procured from Sigma-Aldrich Chemicals Pvt. Ltd., New Delhi. Sodium dodecyl sulphate (SDS) and Triton X-100 were obtained from Merck Limited (Worli, Mumbai) and Sisco Research Laboratories (Mumbai), respectively while, Cetyl trimethylammonium bromide (CTAB) was procured from Amresco (Solon, Ohio, USA). All other chemicals employed were of analytical grade.

Sample preparation

All in vitro experiments with ThT or pyrene were carried out in 20 mM Gly-Gly buffered at pH 8.5. Amyloid fibrils of HEWL obtained by incubation of protein at 333 K in pH 2.7 buffer for 13 days were prepared as reported previously [15]. HEWL aggregates were obtained by incubation of protein at 298 K in pH 12.2 buffer for 8 days as described previously [16]. All experiments were performed at 298 K.

Thioflavin T solution

Stock solution of ThT (~1 mg/ml) in deionized water was filtered through 0.45 μm syringe filter before estimation of the concentration in ethanol using extinction coefficient of 26,620 M^{-1} cm^{-1} at 416 nm [17]. Stock solution was stored at 277 K and used within a month. Assay solutions were prepared by diluting the stock solution in 20 mM, pH 8.5 Gly-Gly buffer.

Fluorescence and absorption measurements

While measuring ThT fluorescence, the final ThT concentration was kept at 20 μM in the medium for all samples. For protein samples, the concentration of protein was kept at 12 μM. Samples were excited at 450 nm (1 nm slit width) and subsequent emission between 470 and 550 nm (5 nm slit width) was detected in photon counting mode using the Jobin-Yvon Fluoromax-3 spectrofluorometer. The background intensity from Raman scatter and ThT free samples were negligible compared to sample fluorescence intensity, these were however subtracted from each measurement. Pyrene fluorescence intensity ratio was used to monitor micelle formation as described previously [18]. Stock solution of pyrene in methanol (HPLC grade) was diluted to 2 μM in presence of different concentrations of surfactant (in pH 8.5 buffer). The ratio of vibronic band intensities (III/I) in pyrene emission was obtained by exciting the samples at 310 nm (1 nm slit width) and collecting emission between 350 nm and 450 nm (1 nm slit width) using Jobin-Yvon Fluoromax-3 spectrofluorometer. The emission spectra shown are averages of three independent measurements. For measuring the absorption spectra, a Varian Cary-100 spectrophotometer employing double beam optics with a cuvette path length of 1 cm was employed.

Mammalian cell culture

HT29 (human colon adenocarcinoma) and BHK-21 (baby hamster kidney) cells obtained from National Centre for Cell Science, India, were maintained in Dulbecco's Modified Eagle's (DMEM) medium supplemented with 10% fetal bovine serum (FBS), 50U/ml penicillin and 50 mg/ml streptomycin in a humidified atmosphere in 5% CO_2 at 37 °C.

Fluorescence microscopy

Fluorescence images were recorded using a laser scanning confocal microscope (LSM 510, Carl Zeiss, Germany) employing the 458 nm Argon line for exciting ThT. The plated cells were washed with PBS (pH 7.4) three times before addition of 50 μM ThT to eliminate fluorescence contributions from the growth media. After addition of ThT, the cells were incubated for 15 min at room temperature before collecting images to allow for partitioning of the dye into the cell. The images were collected under a open pinhole (840 μm) using a 20× objective (0.50 NA) after filtering the emission using a 475–525 nm band pass filter to block excitation photons.

Results and discussion

The interaction between Thioflavin T and surfactants were studied by measuring the electronic absorption spectrum of ThT in the presence of surfactants. Figure 2a shows that in absence of surfactant, ThT displays a λ_{max} around 412 nm in pH 8.5 buffer, consistent with earlier reports [8, 11]. Soon after SDS (0.25 mM) is added in the medium, the peak absorbance drops by ~22% although the peak wavelength remains unchanged. As the SDS concentration is increased further, from 0.5 mM to 2.0 mM, we observe a concomitant rise in the absorbance, while the absorption spectrum shifts to a longer wavelength. As we approach higher SDS concentrations from 2 mM to 5 mM, a degree of saturation is evident in the rising absorbance value. In presence of 5 mM SDS, ThT displays a λ_{max} ~428 nm with a significant increase (~28%) in the peak absorbance in comparison to that observed in pH 8.5 buffer. Figure 2b compares the absorption spectrum of ThT in buffer with those in presence of 5 mM CTAB, 2 mM Triton X-100 and 2 mM Tween 20. No significant change in ThT absorption spectrum is evident in presence of CTAB or Triton X-100 or Tween 20 in sharp contrast to the dramatic changes observed with SDS. All the surfactants employed, namely SDS (cmc ~ 1.3 mM), CTAB (cmc ~ 0.26 mM), Triton X-100 (cmc ~ 0.89 mM) and Tween 20 (cmc ~ 0.081 mM) were observed to form micelles under the conditions employed here. The above cmc values for the surfactants under the conditions employed in ThT experiments were determined using pyrene as probe (see later).

The initial drop in absorbance of ThT on addition of 0.25 mM SDS could arise from formation of premicellar aggregates, where SDS monomers might cluster around oppositely charged ThT [19]. Closer investigations with SDS in the concentration range 20 to 200 μM revealed a gradual dip in ThT absorbance at 412 nm, starting from 0.47 in pH 8.5 buffer to 0.35 in presence of 200 μM SDS,

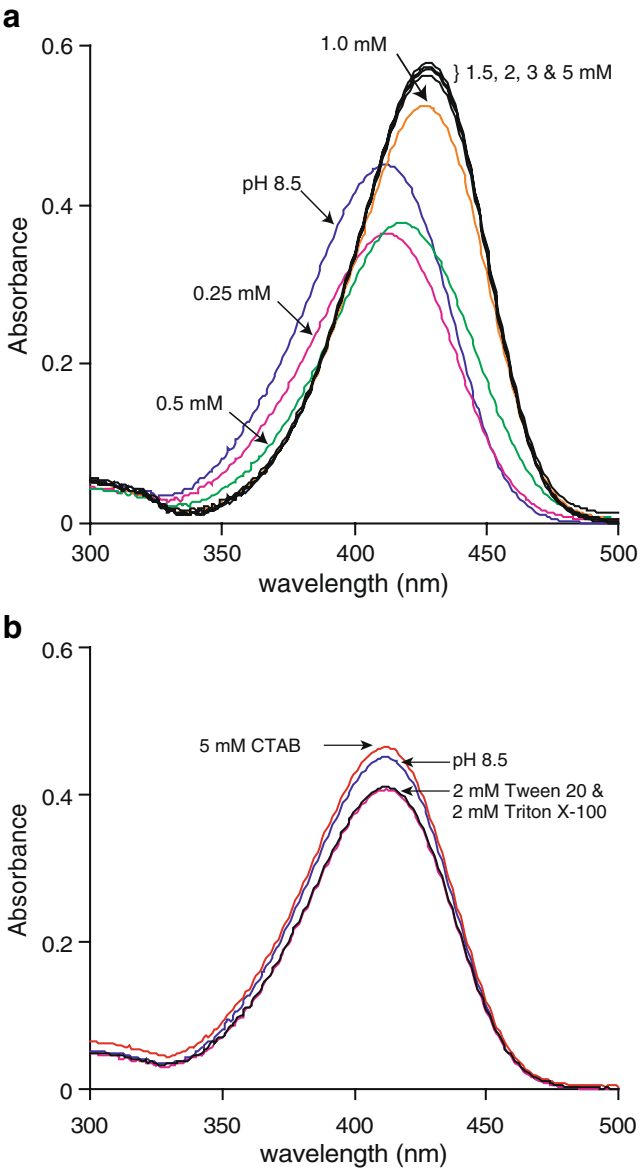

Fig. 2 **a** Absorption spectrum of 20 μM ThT in presence of different concentrations of SDS at 298 K in 20 mM Gly-Gly, pH 8.5 is shown. The curves are: *blue*, in pH 8.5 buffer alone; *magenta*, in 0.25 mM SDS; *green*, in 0.5 mM SDS; *orange*, in 1.0 mM SDS; *black*, 1.5, 2.0, 3.0 and 5.0 mM SDS. **b** Absorption spectrum of ThT in presence of other surfactants is shown. The curves are: *blue*, in pH 8.5 buffer alone; *magenta*, in 2 mM Tween 20; *red*, in 5 mM CTAB and *black*, 2 mM Triton X-100. Other conditions are identical to Fig. 2a

with no observable shift in peak wavelength (see Supplementary data). A similar dip and rise in absorbance with increasing SDS concentration has been observed in cationic pyridoimidazole derivative also [20]. In the absence of any clear isobestic point or shift in peak wavelength these premicellar aggregates are likely to be disordered or nonspecific [19, 21]. The subsequent red-shift and rise in the intensity of the spectrum from 0.5 mM SDS onwards points to increasing micellization of ThT, which appears

complete at 1.5 mM SDS from Fig. 2a. The absorption rises with increase in SDS concentration since the micelles which begin to form may favorably partition the non-polar moieties of ThT into the micellar hydrophobic interior, while the positive charge in ThT may be stabilized by the negative sulphate in the exterior surface. It has been shown that ThT ground state is progressively less stabilized (increasing λ_{max}) as the polarity of surrounding solvent is reduced [11]. For example, the ThT has a λ_{max}~424 nm in $CHCl_3$. Therefore, with a λ_{max}~428 nm, it is likely that a major portion of ThT molecule resides in the non-polar SDS micellar interior.

The absence of any shift in absorption spectrum of ThT in presence of CTAB/Triton X-100/Tween 20 micelles suggests that ThT does not enter inside these micelles. It is interesting to note that ThT clearly discriminates between SDS and other non-anionic micelles in solution on the basis of surfactant charge. Thus, Coulombic attraction, between anionic SDS and cationic ThT and Coulombic repulsion between cationic CTAB and ThT plays a major role in the events shown in Fig. 2a & b. With neutral surfactants like Tween 20 & Triton X-100, there is no Coulombic repulsion, yet no significant change is observable in the absorption spectrum. Perhaps stabilization of the positive charge in ThT is essential for the effective micellization of the probe.

Interaction of Thioflavin T with surfactants was also monitored by measuring ThT fluorescence subsequent to excitation at 450 nm. This wavelength was chosen as it is commonly chosen for monitoring ThT fluorescence in presence of amyloid fibrils. Figure 3a shows the ThT fluorescence intensity at different concentrations of SDS in pH 8.5 buffer. A gradual increase in ThT emission intensity was observed from 0.25 mM SDS to 2 mM SDS. Subsequently the intensity, with λ_{max}~489 nm, remains unchanged from 2 mM SDS to 5 mM SDS, indicating saturation of ThT fluorescence. The emission λ_{max} remained between 484–490 nm, with a single peak, when excitation wavelength was varied between 380–450 nm (data not shown). The excitation spectra were fairly broad, showing a single peak with a λ_{max} between 421–427 nm when emission wavelength was varied between 460–540 nm (data not shown). The λ_{max} for excitation overlaps closely with the λ_{max} for absorption above. Interaction of positively charged ThT with anionic surfactant SDS can be facilitated by both hydrophobic interaction between SDS micelles and ThT, and electrostatic interaction between oppositely charged SDS head group and ThT. The increase in ThT fluorescence with SDS and subsequent saturation may be correlated to micelle formation in SDS as its concentration increases. To verify this, we monitored the micelle formation in SDS using pyrene under conditions identical to that employed in ThT experiments.

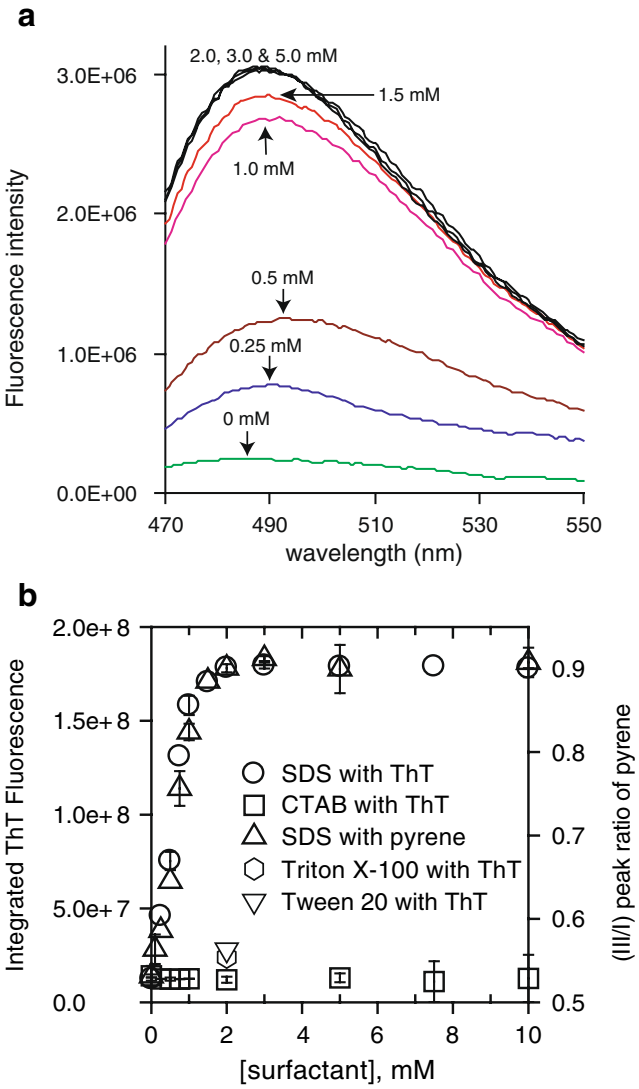

Fig. 3 **a** Change in the fluorescence emission spectrum of 20 μM ThT with different concentrations of SDS in pH 8.5 buffer at 298 K is shown. From bottom to top the [SDS] in curves are: *green*, 0 mM; *blue*, 0.25 mM; *brown*, 0.5 mM; *magenta*, 1.0 mM; *red*, 1.5 mM; and *black*, 2.0, 3.0 and 5.0 mM. **b** Concentration dependent changes in ThT fluorescence and III/I peak ratio of pyrene emission in presence of different surfactants is shown. The symbols are: *circle*, SDS with ThT; *square*, CTAB with ThT; *triangle*, SDS with pyrene; *hexagon* Triton X-100 with ThT; and *inverted triangle*, Tween 20 with ThT. Other conditions are similar to Fig. 3a

Pyrene has been employed as a fluorescence probe to monitor micelle formation. The classic dependence of vibronic band intensity ratios in pyrene monomer fluorescence towards solvent polarity has been used to study microenvironment experienced during the micelle formation. This parameter is an excellent indicator of self-association among surfactant molecules [18]. We used the peak III to peak I vibronic intensity ratio (III/I ratio) in pyrene fluorescence emission to the estimate critical micellar concentration of surfactant under conditions employed by us. Figure 3b indicates the gradual increase

in III/I ratio of vibronic bands as a function of SDS concentration. This value saturates around ~0.9 at 2.0 mM SDS and remains constant thereafter indicating the formation of SDS micelles. Figure 3b also shows the variation of integrated ThT fluorescence with SDS concentration. It is observed that the dependence of pyrene III/I ratio and ThT integrated fluorescence intensity on SDS concentration are nearly superimposable. We can therefore conclude that increase in ThT fluorescence is directly correlated with formation of SDS micelles. The enhanced fluorescence of ThT in presence of SDS micelles can originate from two factors: A) a higher quantum yield owing to a relatively rigid microenvironment in micelle interior compared to solvent and B) a higher ThT molar absorptivity at the excitation wavelength (450 nm) subsequent to micellization. Our observations revealed an approximately three fold increase in fluorescence quantum yield of ThT and a three fold increase in its molar absorptivity at 450 nm. Thus, a nine fold increase in the fluorescence of ThT in presence of SDS is roughly predicted, while the observed increase is about thirteen fold.

Figure 3b shows the change in ThT fluorescence with CTAB concentration. No significant change in ThT fluorescence intensity was observed with CTAB compared to the intensity in aqueous buffers, in the concentration range 0–10 mM. Experiments with pyrene indicated that CTAB was indeed forming micelles as inferred by a constant III/I ratio of ~0.75 beyond 0.25 mM CTAB (data not shown). This indicates that Coulombic repulsion between positively charged CTAB head group and positively charged ThT hinders close interaction of ThT with CTAB micelles. Indeed, electrostatic forces have been previously shown to influence the binding of ThT to fibrils of 13 residue peptides that either contain or do not contain lysine residues [22]. Figure 3b also shows that the increase in ThT fluorescence intensity observed in presence of neutral micelles of Tween 20 and Triton X-100 is relatively insignificant in comparison to that observed with SDS.

ThT is known to display enhanced fluorescence emission at ~480 nm upon binding to amyloid fibrils [4]. We compared the emission profile of ThT in presence of SDS with previously reported amyloid samples of HEWL [15]. Figure 4 compares the emission spectra of ThT in 5 mM SDS, in HEWL incubated in pH 2.7 at 333 K for 13 days (referred to as HEWL sample A) and in HEWL soaked in pH 12.2 at 298 K for 8 days (referred to as HEWL sample B). Presence of amyloid fibrils in HEWL sample A was confirmed by AFM imaging (see image A in Fig. 4). The highest ThT fluorescence intensity is observed in HEWL sample A. An intermediate level of ThT fluorescence was detected with HEWL sample B, where both large globular aggregates (not shown here) and amyloid fibrils (see image B in Fig. 4) were detected by AFM. But interestingly,

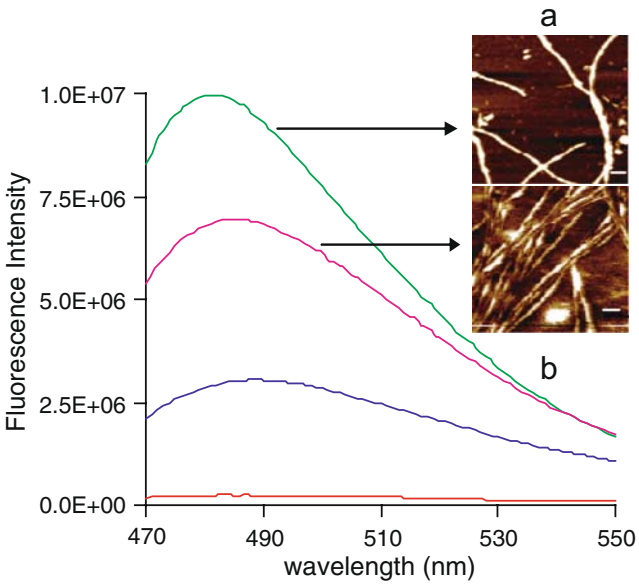

Fig. 4 Fluorescence emission spectra of ThT (20 μM) in 20 mM, pH 8.5 Gly-Gly buffer under different experimental conditions are shown. ThT curves from bottom to top are: *red*, with pH 8.5 buffer only; *blue*, with 5 mM SDS; *magenta*, with 12 μM HEWL previously in pH 12.2 at 298 K for 8 days; *green*, with 12 μM HEWL previously in pH 2.7 at 333 K for 13 days. *Inset*: AFM images of HEWL are shown as follows: (*a*) HEWL in pH 2.7 at 333 K for 13 days and (*b*) HEWL in pH 12.2 at 298 K for 8 days. The scale bar is equivalent to 100 nm. The samples were deposited on fresh cleaved mica surface and images were acquired in air under MAC MODE in Picoplus AFM (Molecular Imaging, USA)

comparatively lower but significant ThT fluorescence was observed in presence of SDS. The wavelength of emission maximum for ThT in HEWL sample A, B and SDS were 482, 485 and 489 nm, respectively. Previous studies could establish no obvious correlation of ThT emission λ_{max} with surrounding solvent properties [10]. The integrated fluorescence intensity of these samples is shown in Table 1. It is

Table 1 Thioflavin T fluorescence in different environments

Thioflavin T (20 μM) in presence of	Integrated fluorescence intensity λ_{ex}=450 nm	Relative fluorescence intensity	r_{ss}[a] λ_{em}=490 nm (SDS) / 484 nm (HEWL)
pH 8.5 buffer	1.35 E+07	1.0	Not determined
0.25 mM SDS	4.59 E+07	3.4	Not determined
5 mM SDS	1.79 E+08	13.2	0.359±0.013
5 mM CTAB	1.30 E+07	~1.0	Not determined
2 mM Triton X-100	2.40 E+07	1.8	Not determined
2 mM Tween 20	2.81 E+07	2.1	Not determined
HEWL pH 2.7	4.87 E+08	36	0.378±0.021
HEWL pH 12.2	3.81 E+08	28	0.355±0.004

[a] r_{ss} refers to steady state fluorescence anisotropy. This was not determined for weakly fluorescent samples as they are prone to errors

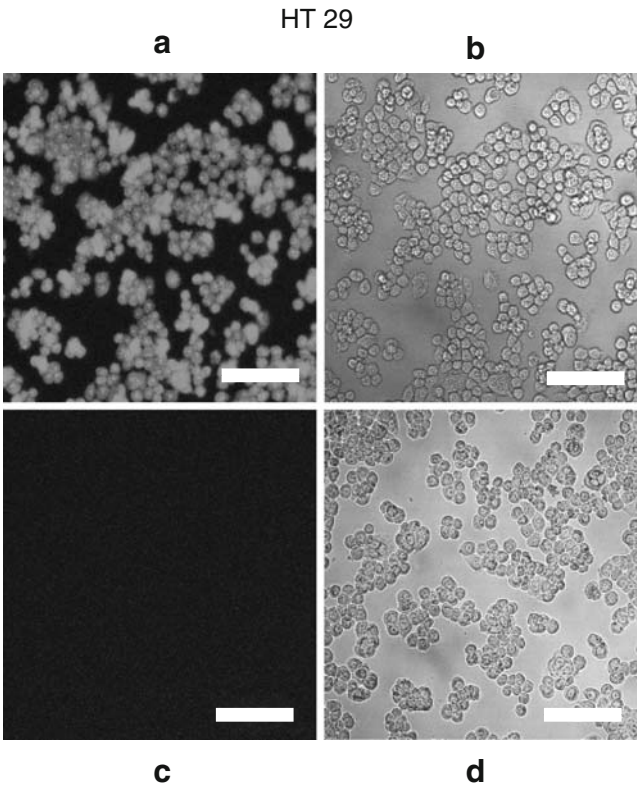

Fig. 5 Fluorescence images of HT-29 mammalian cells are shown in the presence and absence of thioflavin T. Panels **a** and **b** reveal cells with 50 μM thioflavin T, in the fluorescence and bright field mode, respectively. Panels **c** and **d** reveal similar cells without thioflavin T in the fluorescence and bright field mode, respectively. The *scale bar* represents 100 μm

thus understandable that fluorescence enhancement of ThT displays a hierarchy that is possibly related to the viscosity/rigidity in the immediate microenvironment of the probe. It is known that ThT fluorescence intensity increases by more than hundred fold when transferred from water to glycerol [10]. Interestingly, the steady state fluorescence anisotropy of ThT is quite close to 0.4 in presence of HEWL fibrils and SDS (Table 1) suggesting that bound ThT is fairly immobile in these samples. A recent report has highlighted the considerable variability in the rigidity amongst amyloid fibrils from different sources [23].

Micelles are good models of biological membranes. It is therefore possible that the fluorescence of ThT shall be enhanced by the lipid bilayer of the plasma membrane and membrane bound organelles in the cytoplasm of the living cell. We thus proceeded to investigate the fluorescence of ThT in presence of eukaryotic cells BHK-21 (baby hamster kidney cells) and HT29 (human colon adenocarcinoma cells). In Fig. 5, panel a reveals the fluorescence microscopy images immediately after ThT staining of HT29 cells. Panel b in the same figure shows the contour of the same cells under bright field settings. Images (under identical settings) from control samples which had similarly plated cells, but where no ThT was added are shown in panel c (in fluorescence mode) & panel d (in bright field mode). Figure 6 shows the images obtained similarly with BHK-21 cells.

Both BHK-21 & HT29 images reveal ThT fluorescence originating from the cell cytoplasm and nucleus, while no characteristic membrane staining pattern is observed as was anticipated. The ThT dye appears to have made a facile entry into the cell. Inside the cell, it is likely to encounter and bind to a host of components like nucleic acids, membranes and proteins resulting in fluorescence. The bright ThT fluorescence from mammalian cell interiors clearly emphasizes that attempts to detect amyloid-β *in vivo* using ThT (or its derivatives) will require cautious interpretation.

It is likely that significant fraction of ThT shall be present in the extracellular PBS medium, although we observed a fairly dark background outside the cells. This is not surprising because ThT fluorescence is negligible in the aqueous medium. The fluorescence from ThT in the cells was retained for both BHK-21 and HT29 even after washing away the external medium with ThT free PBS, suggesting that ThT is firmly bound inside the cells.

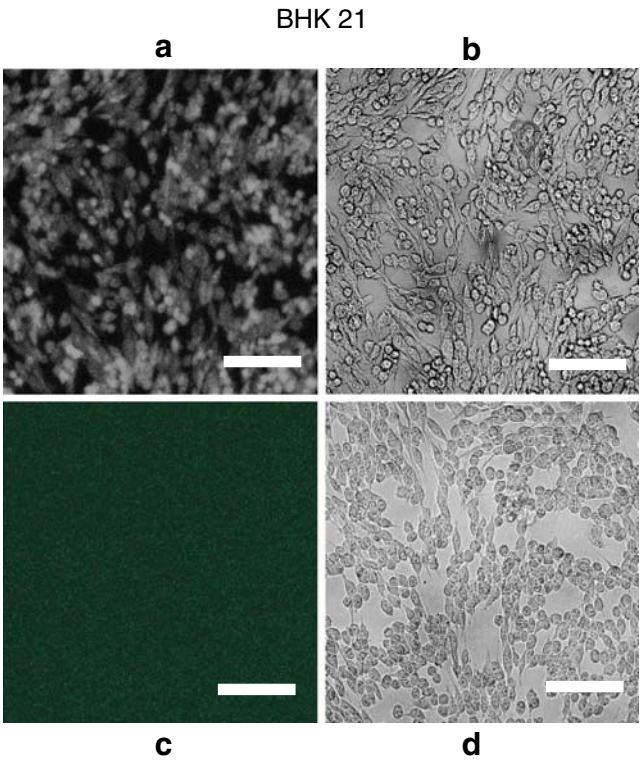

Fig. 6 Fluorescence images of BHK-21 mammalian cells are shown in the presence and absence of thioflavin T. Panels **a** and **b** reveal cells with 50 μM thioflavin T, in the fluorescence and bright field mode, respectively. Panels **c** and **d** reveal similar cells without thioflavin T in the fluorescence and bright field mode, respectively. The *scale bar* represents 100 μm

Thioflavin T has been earlier employed for staining human reticulocytes for flow cytometric analysis of blood samples [24] and recently with K562 leukemia cells [25]. The negative charge on the phosphate in the polar phospholipid headgroup in the membrane is likely to facilitate the entry of ThT into the cell based on our results with SDS. However, the mechanism of ThT entry into the cell is not clear at the moment. Nevertheless, ThT appears as a promising dye to label and stain biological cells chiefly due to the fact that free ThT in the extracellular medium is practically non-fluorescent rendering a sharp contrast in the cell fluorescence images while obviating the need to wash excess free dye from cell medium to improve contrast.

Conclusions

We have shown that Thioflavin T dye prefers to selectively reside inside anionic micelles like SDS instead of cationic & neutral micelles. Inside SDS micelles, the absorption peak wavelength of ThT is red shifted by 16 nm with ~28% increase in peak molar absorptivity. The fluorescence emission from ThT is enhanced by more than one order of magnitude inside SDS micelles, primarily due to increases in molar absorptivity and fluorescence quantum yield. ThT can prove useful as a membrane permeant dye to fluorescently label mammalian cells and selectively label anionic micelles.

Acknowledgements We thank Mr. Vijay Kumar Ravi for the AFM images and Mr. P. Gopinath for assisting in the recording of the fluorescence images.

References

1. Vassar PS, Culling CFA (1959) Fluorescent stains with special reference to amyloid and connective tissues. Arch Pathol 68:487–498
2. Saeed SM, Fine G (1967) Thioflavin-T for amyloid detection. J Clin Pathol 47(5):588–593
3. Naiki H, Higuchi K, Hosokawa M, Takeda T (1989) Fluorometric determination of amyloid fibrils in-vitro using the fluorescent dye, thioflavin T1. Anal Biochem 177(2):244–249
4. LeVine H III (1993) Thioflavin T interaction with synthetic Alzheimer's disease β amyloid peptides: detection of amyloid aggregation in solution. Protein Sci 2(3):404–410
5. Canete M, Villanueva A, Juarranz A, Stockert JC (1987) A study of interaction of thioflavine T with DNA: evidence for intercalation. Cell Mol Biol 33(2):191–199
6. Ilanchelian M, Ramaraj R (2004) Emission of thioflavin T and its control in the presence of DNA. J Photochem Photobiol A 162 (1):129–137
7. Raj CR, Ramaraj R (1999) Influence of cyclodextrin complexation on the emission of thioflavin T and it's off-on control. J Photochem Photobiol A 122(1):39–46
8. Voropai ES, Samtsov MP, Kaplevskii KN, Maskevich AA, Stepuro VI, Povarova OI, Kuznetsova IM, Turoverov KK, Fink AL, Uverskii VN (2003) Spectral properties of thioflavin T and it's complexes with amyloid fibrils. J Appl Spectrosc 70(6):868–874
9. Stsiapura VI, Maskevich AA, Kuzmitsky VA, Turoverov KK, Kuznetsova IM (2007) Computational study of thioflavin T torsional relaxation in the excited state. J Phys Chem A 111 (22):4829–4835
10. Friedhoff P, Schneider A, Mandelkow EM, Mandelkow E (1998) Rapid assembly of Alzheimer-like paired helical filaments from microtubule-associated protein tau monitored by fluorescence in solution. Biochemistry 37(28):10223–10230
11. Maskevich AA, Stsiapura VI, Kuzmitsky VA, Kuznetsova IM, Povarova OI, Uversky VN, Turoverov KK (2007) Spectral properties of thioflavin T in solvents with different dielectric properties and in a fibril-incorporated form. J Proteome Res 6 (4):1392–1401
12. Kelenyi G (1967) On the histochemistry of azo group-free thiazole dyes. J Histochem Cytochem 15(3):172–180
13. Yamamoto S, Hasegawa K, Yamaguchi I, Tsutsumi S, Kardos J, Goto Y, Gejyo F, Naiki H (2004) Low concentrations of sodium dodecylsulfate induce the extension of β_2-microglobulin-related amyloid fibrils at a neutral pH. Biochemistry 43(34):11075–11082
14. Rangachari V, Reed DK, Moore BD, Rosenberry TL (2006) Secondary structure and interfacial aggregation of a amyloid-β 1(–40) on sodium dodecylsulfate micelles. Biochemistry 45 (28):8639–8648
15. McAllister C, Karymov MA, Kawano Y, Lushnikov AY, Mikheikin A, Uversky VN, Lyubchenko YL (2005) Protein interactions and misfolding analyzed by AFM force spectroscopy. J Mol Biol 354(5):1028–1042
16. Homchaudhuri L, Kumar S, Swaminathan R (2006) Slow aggregation of lysozyme in alkaline pH monitored in real time employing the fluorescence anisotropy of covalently labeled dansyl probe. FEBS Lett 580(8):2097–2101
17. Wall J, Murphy CL, Solomon A (1999) In vitro immunoglobulin light chain fibrillogenesis. Methods Enzymol 309:204–217
18. Kalyanasundaram K, Thomas JK (1977) Environmental effects on vibronic band intensities in pyrene monomer fluorescence and their application in study of micellar systems. J Am Chem Soc 99 (7):2039–2044
19. Maiti NC, Mazumdar S, Periasamy N (1998) J- and H-aggregates of porphyrin-surfactant complexes: time-resolved fluorescence and other spectroscopic studies. J Phys Chem B 102(9):1528–1538
20. Krishnamoorthy G, Dogra SK (2000) Effect of micelles on the prototropic equilibrium of 2-(4'-N,N-dimethylaminophenyl) pyrido [3,4-d] imidazole. Phys Chem Chem Phys 2:2521–2528
21. Maiti NC, Mazumdar S, Periasamy N (1996) Controlled J-aggregation of porphyrins by cationic surfactants. Curr Sci 70 (11):997–999
22. Khurana R, Coleman C, Ionescu-Zanetti C, Carter SA, Krishna V, Grover RK, Roy R, Singh S (2005) Mechanism of thioflavin T binding to amyloid fibrils. J Struct Biol 151(3):229–238
23. Knowles TP, Fitzpatric AW, Meehan S, Mott HR, Vendruscolo M, Dobson CM, Welland ME (2007) Role of intermolecular forces in defining material properties of protein nanofibrils. Science 318 (5858):1900–1903
24. Sage BH Jr, O'Connell JP, Mercolino TJ (1983) A rapid, vital staining procedure for flow cytometric analysis of human reticulocytes. Cytometry 4(3):222–227
25. Darghal N, Garnier-Suillerot A, Salerno M (2006) Mechanism of thioflavin T accumulation inside cells overexpressing p-glycoprotein or multidrug resistance-associated protein: role of lipophilicity and positive charge. Biochem Biophys Res Commun 343 (2):623–629